Chem Soc Rev

The electron's spin and molecular chirality- How are they related and how do they affect life processes?

SCHOLARONE™
Manuscripts

The electron's spin and molecular chirality- How are they related and how do they affect life processes?

Karen Michaeli,[a] Nirit Kantor-Uriel,[b] Ron Naaman,*[b] David H. Waldeck[c]

a) Department of Condensed Matter Physics, Weizmann Institute, Rehovot 76100, Israel

b) Department of Chemical Physics, Weizmann Institute, Rehovot 76100, Israel

c) Department of Chemistry, University of Pittsburgh, Pittsburgh, Pennsylvania 15260, USA

Abstract

The recently discovered chiral induced spin selectivity (CISS) effect gives rise to a spin selective electron transmission through biomolecules. Here we review the mechanism behind the CISS effect and its implication for processes in Biology. Specifically, three processes are discussed: long-range electron transfer, spin effects on the oxidation of water, and enantioselectivity in bio-recognition events. These phenomena imply that chirality and spin may play several important roles in biology, which have not been considered so far.

1 Introduction

The term chirality, which derives from the Greek 'cheir' for hand, is used to describe a molecule's or a material's lack of parity symmetry; namely, it has no inversion symmetry and a mirror symmetry operation transforms one enantiomer into the other.[1] Interestingly, many biomolecules are chiral and its ubiquity suggests that it may offer some benefit for Life. As many biochemical reactions involve chiral molecules, much effort has been placed on understanding enantioselectivity in chemical transformations[2,3,4] and the physicochemical properties of chiral molecules.[5] However, it remains unclear as to why Nature has preserved chirality so persistently, despite the energy cost of keeping molecules chiral. The energy cost results from the lower entropy associated with selecting one enantiomer out of the chiral possibilities. This review focusses on possible benefits for its preservation, which arise from the interaction of the electrons' spin with the electronic potential of chiral molecules.

The development of quantum mechanics in the 1920's has transformed our understanding of chemistry. Notably, the notion of electron spin was unexpected and introduced radically new concepts into physics. The ideas of quantum mechanics (quantization, wave functions, and probability density) and the symmetry constraints associated with spin and the Pauli principle were integrated into a comprehensive description of matter during the twentieth century. While two electrons always repel each other as in classical electrostatics, the indistinguishability of electrons gives rise to an exchange energy in quantum mechanics that changes with the electron spin; two electrons whose charge distribution share a region of space (or orbital overlap) have an electrostatic repulsion energy that depends on whether their spins are parallel or anti-parallel. In addition, the spin concept has proved to be particularly important for understanding molecules with unpaired electrons, materials with high spin-orbit coupling (SOC), and the multiplet structure of spectra (energy splitting in general).

In 1999 it was first reported that the probability of electron transmission through chiral molecules depends on the electron spin, an effect which has been called chiral induced spin selectivity (CISS).[6] Depending on the handedness of the molecule, electrons of a certain spin can traverse the molecule more easily in one direction than in the other. These directions are reversed for electrons of opposite spin. Since that time, a number of different chiral organic molecules and biomolecules have been shown to act as spin filters, of which some of the most selective spin filters are nucleic acids[7,8] and peptides.[9] These observations are surprising, because spin filtering

is commonly associated with magnetic materials or with substances that possess large spin orbit couplings (SOCs), rather than organic molecules which are typically neither magnetic nor have large SOC. Since its discovery, the effect has been observed experimentally and verified in different systems.[10-15]

A number groups have worked to construct a theoretical framework for describing the CISS effect;[16-25] however, many of these proposals rely on an SOC which is much larger than that typically observed in organic molecules. Recent work[26] has shown that the helical geometry of a molecule can couple the electron spin direction and their velocity so that electrons moving in one direction have one preferred spin alignment and those moving in the opposite direction have the opposite preferred spin alignment. While the spin-orbit coupling alone is too weak to account for the CISS effect, in combination with a dipole electric field it can lead to strong spin-dependent transmission at room temperature. Such a dipole potential is known to appear in many chiral molecules and it prevents electronic states from delocalizing throughout the system. As a consequence, the transmission through these molecules occurs via quantum tunneling, either direct or in several steps as in the case of hopping conductivity. Michaeli's theoretical model[26] implies that the CISS effect is significant whenever electrons transfer via tunneling with low transmission probability. Furthermore, it predicts that the helicity-induced SOC gives rise to a tunneling probability that is several orders of magnitude larger than in achiral molecules (see Figure1). Hence, the coupling of the electron spins to their linear momenta by the helicity-induced SOC enhances the transmission through the molecules. This mechanism suggests that electron backscattering by vibrational modes is suppressed, as it requires a change in spin as well as in linear momentum. This weak coupling to vibrational modes ought to inhibit inelastic collisions and energy loss, as heat.

Figure 1 presents the transmission probability and the spin polarization calculated by this theoretical model.[26] In this calculation, the electrons are tunneling from an electron source to an electron drain by way of a chiral potential, across which a bias voltage is applied. The transmission probability is larger for chiral structures versus achiral ones, by 10 to 100 times over the voltage range shown. Figure 1A shows that the electron tunneling probability increases systematically with the strength of the SOC and the applied voltage. Panel B shows the spin polarization that is calculated for a chiral molecule with four different lengths. The calculation predicts that the spin polarization increases as the molecular length increases, as indeed was

observed experimentally,[7,27] and it varies with bias potential. The model predicts spin polarization values of 60% to 70% for a 10 meV SOC, which is about the value of SOC for carbon atoms.
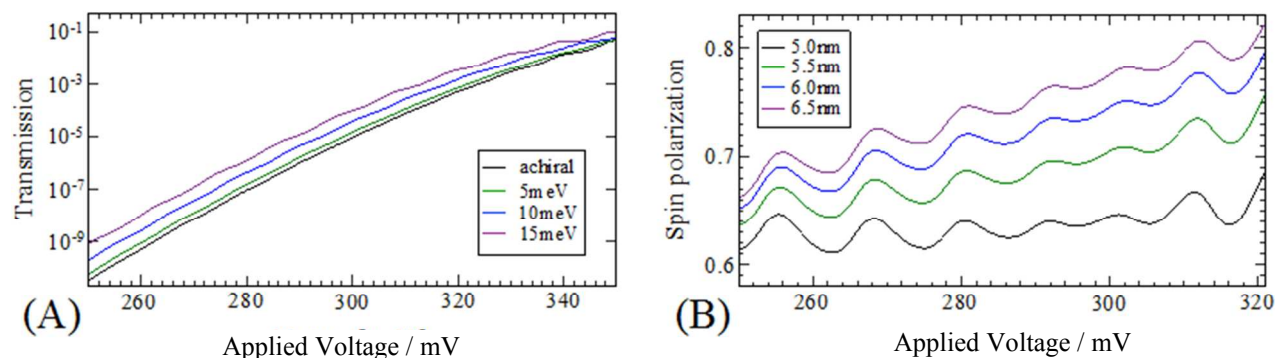

Figure 1: The transmission probability and spin polarization, calculated based on the theoretical model, are plotted as a function of the applied voltage. Panel (A) illustrates the significant difference in transmission probability between achiral (black curve) and chiral molecules with different strengths of SOC (green curve - 5meV, blue curve - 10meV, purple - 15meV). Panel B shows the spin polarization for electrons traversing chiral molecules of different length but with the same SOC (10meV) and a dipole field of 7.5×10^7 V/m. This plot illustrates that spin polarization increases with length, even though the total transmission is suppressed.

The theory points to the importance of the molecular dipole moment and/or the electric field that is applied on the molecules for observing a large CISS effect. This finding rationalizes why the spin polarization observed for electron scattering from gas phase molecules is so much weaker than that of molecules in ultrathin films, of order 10^{-5} rather than 10^{-1}.[28] For an isotropically oriented collection of gas phase dipolar molecules, the average dipole moment of the ensemble is zero even though each molecule has a non-zero dipole moment. In the same manner, the dissymmetry in the electron scattering, which is linked to the dipole moment of the chiral gas phase molecules, averages to zero for an isotropic collection of such molecules. While other terms, such as the pure SOC, do not average to zero. Hence, the magnitude of the dissymmetry in the scattering effect becomes extremely small.

The CISS effect implies that the electronic states in these chiral molecules have a well-defined helicity. In other words, although time reversal symmetry is not broken (no magnetic field is applied), the projection of spin onto the propagation direction for all electrons has the same sign, which depends on the handedness of the molecule. One-dimensional helical states have attracted much attention recently in condensed matter physics, where they appear at the

edge of two-dimensional topological insulators.[29] Similar to the chiral molecules, the origin of this phenomenon arises from the absence of parity symmetry, and the resulting SOC. In the topological insulators, the unique properties of the insulating bulk give rise to the perfectly helical edge states that are protected from backscattering. In contrast for chiral molecules the states are only quasi-helical and robustness is only achieved in the presence of a dipole field.

Below we discuss three aspects of the spin filtering in relation to biomolecules and elaborate how the CISS effect impacts their function. In part, these properties may be the reason why evolution has conserved chirality so strictly.

2   Efficient electron transfer

The design features of artificial organic conductors are closely related to the electronic and structural features of well-known metallic conductors and semiconductors. Namely, they involve delocalized electronic states and a narrow band-gap, a small energy difference between the highest occupied molecular orbital (HOMO) and the lowest unoccupied molecular orbital (LUMO), which allows the ready promotion of carriers into partly filled states – either thermally or through doping. In Biology, however, electron transfer (ET) processes do not take place through conjugated molecules, but rather ET occurs primarily in and through proteins; for example, in photosynthesis and in respiration. Why are proteins preferred over conjugated systems?

Experimental studies of electron transfer show that the rate constant k_{ET} can be described by exponential distance, L, dependence, $k_{ET} \propto \exp(-\beta L)$ where β is the damping constant, and this behavior is commonly interpreted as superexchange mediated tunneling. Theoretical work suggests that electron transfer through chiral systems can be enhanced over that through achiral molecules of similar length and composition by 10 to 100 times; see Fig 1A. Several chiral systems that were investigated in detail show an efficient electron transfer rate beyond what is expected for saturated hydrocarbons of the same contour length. For example, it was found that when electrons are transferred through α-helical oligopeptides, the electron transfer rate damping constant, β, can be as low as 0.1 per angstrom,[30-32] whereas the value found for saturated hydrocarbons is of about 0.9 to 1.0 per angstrom.[33,34] In proteins, however, the damping constants are found to be somewhat larger; in β sheets the damping constant lies between 0.9 and 1.2 Å^{-1} and in α helices it ranges from 1.25 to 1.6 Å^{-1}.[35] Despite amazing progress over the past

few decades, our mechanistic understanding of electron transfer process through peptides and proteins remains limited.[36-38]

   Only recently have workers begun to consider the importance of a peptide's chirality on the underlying nature of its electron transfer behavior. In particular, they have examined spin selectivity in charge transport and charge transfer. For achiral molecules, such as alkanethiols, it is found that no spin polarization is present; whereas polyalanine, as well as other helical peptides, have been shown to display spin selectivity by a number of different methods, including photoemission, electrochemical charge transfer, Hall probe measurements, and tunneling current measurements.[9,39,40] In addition to polypeptides, spin selectivity has been demonstrated in the transmission of electrons through duplex DNA[7] and through the protein, bacteriorhodopsin.[41]
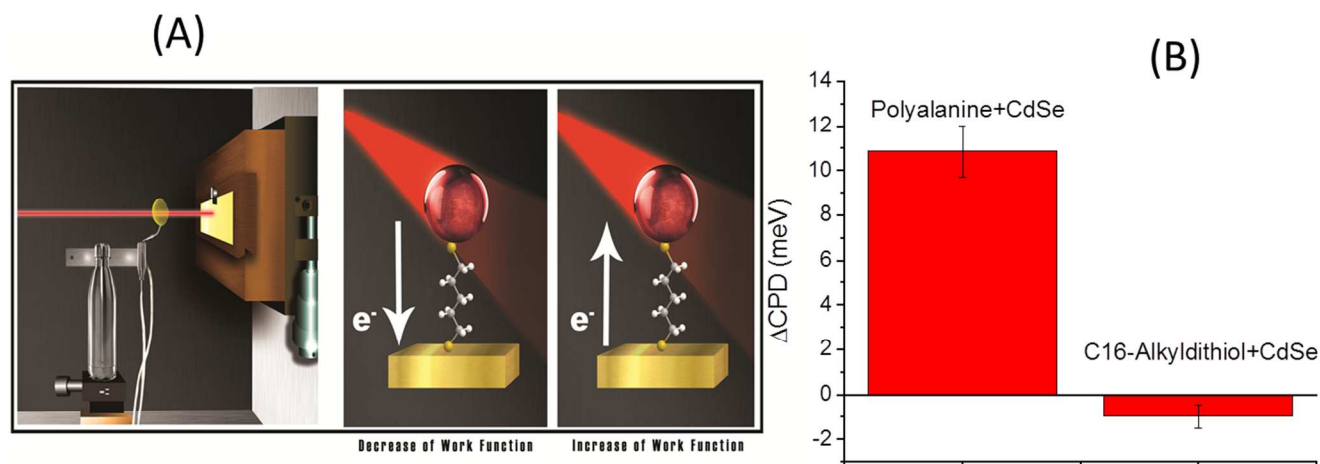

Figure 2: (A) The Kelvin probe set-up for measuring the change in the surface's work function upon illumination is illustrated. The left panel shows the experiment design in which a gold reference plate oscillates relative to the substrate, which is coated with a self-assembled monolayer (SAM) of the organic molecules, on top of which CdSe nanoparticles (NPs) are attached. When the NPs are excited by light, an electron may transfer to the substrate (middle figure) and then the measured work function will decrease; alternatively, the electron may be transferred from the substrate to the NP (right panel) and then the work function will increase. (B) The bar chart compares the measured change in the workfunction when it is normalized to the molecular length, ΔCPD, for the polyalanine or for the hexadecanedithiol.

   In a recent experiment, we compared the photoinduced charge transfer in a chiral oligopeptide to that of a shorter alkanethiol. Figure 2 shows the experimental design, in which a self-assembled monolayer of dithiols is adsorbed on a gold electrode and CdSe nanoparticles are attached to the top of the monolayer. Using the Kelvin probe method, the change of the

assembly's work function was measured upon illumination that is resonant with the exciton transition of the CdSe. The change in the work function is proportional to the change in the dipole moment across the monolayer film, namely to the steady-state amount of charge that is transferred from the nanoparticles to the substrate times the film thickness (length of the molecule). If an electron is transferred from the nanoparticles to the substrate, then the surface workfunction decreases; however if a hole is transferred to the substrate then the workfunction increases.

This experiment compares the charge transfer through polyalanine with 14 amino acids, which is about 2.3 nm long, with that of hexadecane dithiol, $HS-(CH_2)_{16}-SH$, which is about 2 nm long. To compare the workfunction shifts for the two assemblies, the observed changes in the workfunction were divided by the length of the molecules to generate the quantity ΔCPD, which is in V/nm. As shown in Fig 2B, the ΔCPD for the chiral polyalanine is an order of magnitude larger than is that through the achiral alkanethiol. In addition, the ΔCPD is of opposite sign, indicating that while in polyalanine hole transfer from the nanoparticle is more efficient than electron transfer, the opposite is the case for the alkanethiols. These results are consistent with several studies reported recently, which show a surprisingly efficient electron transfer through biomolecules.[42-44]

To date, most explanations for the enhancement in the range of electron transfer (and transport) through oligopeptides has relied on the consideration of additional noncovalent tunneling pathways (e.g., hydrogen bond contacts) or electron hopping via localized states associated with the amide bonds. Given the clear observations of spin polarization in the electron transmission through polypeptides, it is worthwhile to consider what role it may play in promoting long range charge transfer. For example, the 'tunneling time[45] increases with length and thus one expects that inelastic tunneling effects will become more important with the tunneling distance; however, the likelihood of backscattering should be suppressed for chiral molecules over achiral ones making the overall transfer more efficient for chiral molecules. Unexplored mechanisms of this sort could contribute to the tunneling probability and may function as another way to control the direction and rate of charge transfer.

It is important to note that even if only one spin orientation is transferred; all photoexcited electrons can be transferred. When an electron is excited from a singlet ground state, a singlet excited state is formed in which the electrons' spins are paired; alignments are

anti-correlated. However, in the laboratory frame, the spin of each electron has the same probability to be in any direction. Given enough time the excited electron will be in the right orientation to be transferred through the chiral system. Hence, in principle all excited electrons, or holes, can be transferred through a chiral bridge.

3 Spin selectivity in photoredox reactions

Many reactions in biology require the transfer of multiple electrons, such as for oxygen formation in the photosynthetic system and respiration. In the photosynthetic system, water is split to generate oxygen and protons with a quantum efficiency of about 90%.[46,47] The splitting of water into hydrogen and oxygen, has been investigated extensively as a possible 'clean' energy source.[48-50] Although water electrolyzers and photodriven electrolysis have been demonstrated and devices are commercially produced, its widespread implementation requires additional significant improvements in efficiency. Two related drawbacks of the artificial photodriven formation of oxygen are i) the high overpotential (*circa* 0.5 V) required to initiate the reaction for the oxygen evolution reaction at the photoanode and ii) the non-selectivity of the oxidation, which results in the production of hydrogen peroxide. In addition to improving device efficiencies, overcoming these limitations in the artificial system may provide insights into the analogous bio-processes.

3.1 Spin polarization in photosystem I

A recent study shows that photoinduced electron transfer in the photosystem I complex (PSI) proceeds in a spin polarized[51] fashion. Electron transfer in PSI involves photo-excitation to produce a singlet excited state of the primary electron donor P700, after which, an electron transfers from the heterodimer to the primary acceptor, chlorophyll *a* (A_0), and then to a tightly bound phyloquinone molecule (A_1); see Figure 3. The terminal acceptors in PSI consist of a series of three [4Fe-4S] clusters: F_X, F_A, and F_B . The kinetics of these electron transfer processes has been intensively studied.[52-55] The robust PSI, used in these experiments, is isolated from the thylakoid membranes of cyanobacteria and is stable and active when adsorbed in a dry environment. Earlier studies showed that the adsorbed PSI is in its native form and displays photoinduced electron transfer.[56] In order to assess the spin selectivity in this process, PSI-based monolayers were adsorbed onto the surface of a novel spintronic/capacitance device.[57]

This capacitance device (see Figure 3) senses the spin polarization by monitoring the electrical potential that is generated between a magnetized nickel electrode and an ultrathin silver electrode, which are arranged in a metal-insulator-metal (MIM) structure. When photosensitive molecules, in this experiment PSI assemblies, are placed on top of the silver electrode and are excited by light they can transfer charge with the Ag electrode and generate a photopotential.
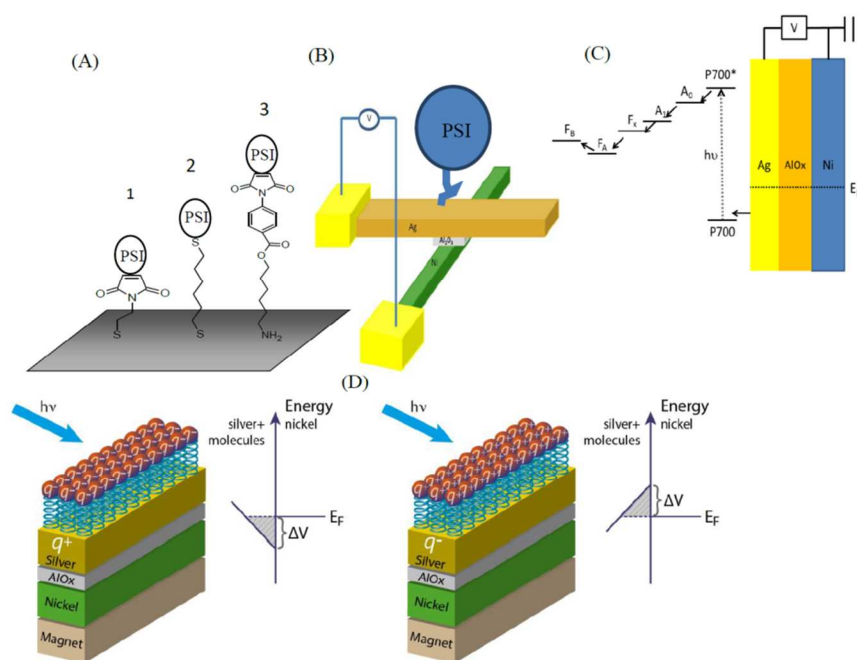

Figure 3: (A) The linkers: 1. DTME; 2. 1,6 hexanedithiol; 3. 6-amino-1-hexanethiol coupled to sulfo-MBS. **(B)** The capacitance device used for monitoring ET and spin selectivity. **(C)** Energy level diagram for the electron transfer when the donor (P700) is located near the silver substrate. From each stage in the electron transfer process, electrons can decay back to P700 and charge recombination can occur. The excitation is proportional to the light intensity and the ratio between the charge separation and the recombination rates define the amount of charge located on the acceptor (FB). The voltage, V, measured between Ni and Ag, is proportional to the amount of electrons transferred from Ag to the oxidized P700. **(D)** A scheme of the device and its energy states. On the right- If the donor (P700) is at the far end of the complex, an electron is transferred to the silver. At steady state, a dipole is formed with its negative pole on the silver and states above the Fermi level of the system are populated (gray area). If the electrons are spin aligned, they can be transferred to the nickel, only if the unpopulated states on the nickel, near the Fermi level, belong to this spin orientation. Otherwise, they will not be transferred and a higher voltage will be measured between the nickel and the silver. On left- If the donor group is placed near the

silver substrate, upon photoexcitation electrons are transferred from the silver to the acceptor and at steady state a dipole is formed with its positive pole on the silver. If the transferred electrons are spin polarized, the empty states below the Fermi level of the system all belong to one spin state. Hence, if the nickel is magnetized so that its electrons are spin polarized and they can tunnel to the silver layer, the voltage will be low, while if it is magnetized in the opposite direction the measured voltage will be higher. I. Carmeli, K. S. Kumar, O. Hieflero, C. Carmeli, R. Naaman, *Angew. Chemie* 2014, 53, 8953. Copyright Wiley-VCH Verlag GmbH & Co. KGaA. Reproduced with permission.

If the charge transfer is spin selective, then the electric potential between the nickel and silver layers will depend on the direction of magnetization of the nickel, because the magnetized nickel has its spin sub-bands filled to different extents. When the minority sub-band electrons have their spins aligned with the same spin polarization as the excess electrons in the silver, the tunneling of an electron from the Ag to the Ni through the AlO_x is more facile than if the electron spins and the minority sub-band electrons are aligned in the opposite direction, as there are fewer acceptor states in the latter case. This difference in tunneling probability creates a difference in photopotential for different magnetizations of the Ni. By measuring the photovoltage for the two different magnetic field directions and comparing it to the case of no magnetic field, the spin polarization in the photoinduced electron transfer can be measured. Of course, the magnitude of the potential difference is reduced by spin depolarization in the Ag. More about the method can be found in reference.[57]

Figure 4 shows data for the photovoltage as a function of the magnetic field direction for the PSI complex assembled on the MIM device. Figure 4A shows the case where the P700 is closer to the substrate than is the acceptor F_B so that an electron is transferred from the Ag layer to the P700, making the Ag positively charged, and Figure 4B shows the case where the iron-sulfur clusters (F_B and F_A) are closer to the silver substrate than is the P700, so that an electron is transferred to the Ag, making it negatively charged. When P700 is close to the substrate (Fig 4A), the surface photovoltage measurements show an increase in the silver's work function of about 10 meV upon illumination (see Fig 4Aiii), consistent with positive charging of the Ag; i.e, electron transfer from the Ag to the P700. The spin dependence of the electron transfer is shown by the magnetic field response (blue arrows in Figure 4Aii) for the MIM structure; the magnitude of the potential changes with the magnetic field direction range from about 0.62 µV to 0.57 µV. Figure 4B shows the case where the FeS clusters were placed closer to the silver surface than the

P700, so that the photogenerated electrons are transferred from the FeS clusters to the silver. In this case the photopotential is negative (Fig 4biii) and comparable in size to the case in panel A. The spin dependence of the electron transfer is revealed by the magnetic field dependence of the photovoltage in the MIM structure; it has a value between -0.30 µV and -0.31 µV (Fig 4bii). The dependence of the photopotential on the external magnetic field and the change in the sign of the magnetic field dependence with injection of holes versus electrons provide good evidence that the charge transfer is spin polarized.
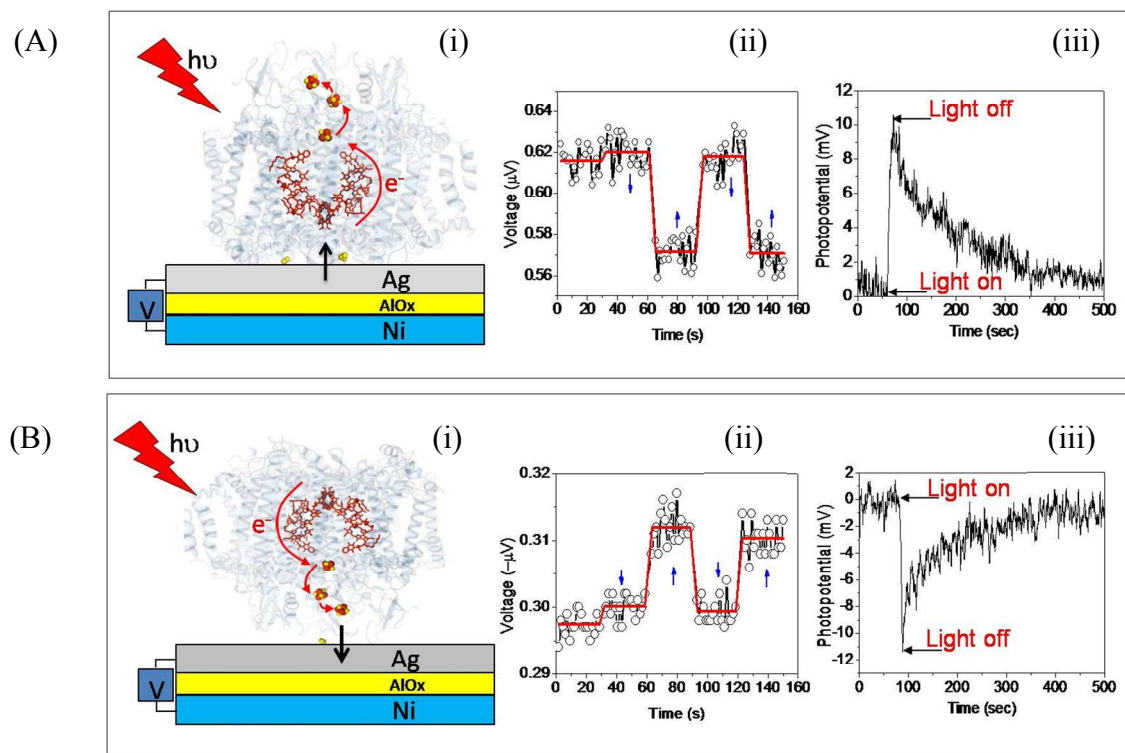

Figure 4: The two configurations studied (4i). Panel A shows PSI adsorbed so that the donor group, P700, is close to the surface, and panel (B) shows PSI adsorbed so that the iron-sulfur clusters (the acceptors) are located near the surface. In 4ii, the voltage measured across the MIM device is shown when the magnetic field is aligned parallel or untiparallel relative to the surface normal (up and down, blue arrows, respectivly). In 4iii the photovoltage signal is shown, as measured with a Kelvin probe placed above the monolayer film/Ag surface, analogous to that shown in Figure 2. The positive and negative signals indicate increases or decreases in the workfunction upon illumination, respectively. I. Carmeli, K. S. Kumar, O. Hieflero, C. Carmeli, R. Naaman, *Angew. Chemie* 2014, **53**, 8953. Copyright Wiley-VCH Verlag GmbH & Co. KGaA. Reproduced with permission.

If we define the spin polarization as the difference in the voltage measured with the Ni magnetic dipole pointing either towards or away from the surface divided by the voltage measured with no magnetic field applied, then

$$P = \frac{V_{H\uparrow} - V_{H\downarrow}}{V_{H=0}}$$

If one uses the raw data to calculate the spin polarization, a value of P = -8 ±1% is found for the P700 near the surface and a value of P = 4 ± 1% is found when the FeS cluster is close to the surface. Because the timescale of the measurement is fairly long, as compared to the spin depolarization time in the Ag layer, the values calculated in this way are smaller than that which would be found if the Ag did not undergo spin depolarization.

References 51 and 57 discuss a procedure that corrects for the loss of spin orientation in the silver and for the nickel not being an ideal spin injector, and their corrected spin polarizations are P = -80 ±20% when P700 is closer to the Ag surface and P = 40 ± 10% when the FeS clusters are closer to the Ag surface. Given that the electrons are transferred "away" from the surface in the first case and are transferred toward the surface in the second case, these results indicate that the spin of the transferred electrons is aligned parallel to their velocity, rather than anti-parallel. The spin polarization observed here demonstrates the spin selectivity in the electron transfer of PSI. The results indicate that an electron that leaves the P700 donor has a well-defined spin alignment in the molecular frame (Figure 4A) and the electrons arriving at the acceptor are also polarized (Figure 4B), albeit somewhat less. The high spin polarization found in this system is consistent with earlier works[58,59,60] which reported spin polarization in EPR measurements. However, in past studies the EPR signal most probably results from biradicals that are formed in the first stage of the electron transfer process. It is noteworthy that the high spin polarization values observed exceed those measured for electron transfer through a 78 base pair DNA duplex with the same device.[57] The efficient electron transfer and the high degree of spin polarization are consistent with the CISS effect.

3.2 Artificial water splitting

While researchers have achieved great success with hydrogen production in photoelectrochemical water splitting, the photoanodic decomposition of water to form O_2 has proved to be more challenging. Oxygen generation has been postulated to occur by different possible mechanisms, however they all involve an OH intermediate. Under basic conditions, oxidation process can occur through two paths. The first is a four-electron process in which O_2 is produced directly, and it is the thermodynamically favored. The other path involves the

formation of a hydrogen peroxide intermediate, which is thermodynamically less favorable, but has a lower activation barrier and therefore is kinetically favored.[61] Note that the formation of the peroxide intermediate may also result in parasitic oxidation processes that reduce cell efficiency.

Figure 5 shows these two possible paths for the water splitting. The unpaired electrons of the two OH radicals can be aligned anti-parallel (Fig. 5A) or parallel (Fig. 5B) in the laboratory frame. When anti-parallel, they react on a singlet surface that correlates with the formation of hydrogen peroxide and they have a barrier for forming the oxygen molecule in its triplet ground state. If the spins of the two radicals are aligned parallel, however, the system is on a triplet potential energy surface and the oxygen molecule product is favored.
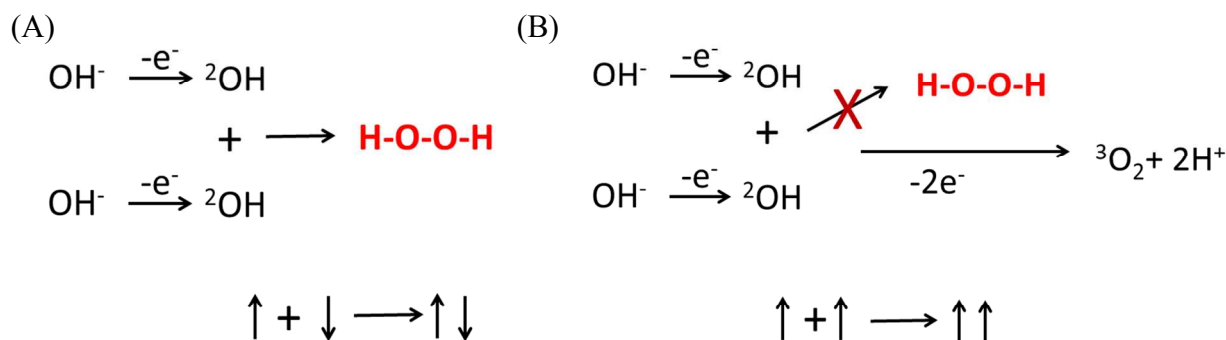

Figure 5: (A) The reaction path occurring when the two spins of the reacting OH radicals are anti-parallel (i.e., paired). In this case formation of hydrogen peroxide is more favorable. (B) When the two spins are parallel the reaction occurs on the triplet surface and diatomic oxygen is favored.

To examine this hypothesis, Mtangi et al.[62] coated a photoanode for water splitting with chiral molecules in order to spin filter the photogenerated electrons, so that the photogenerated OH radicals are spin polarized. Indeed, they found that the photoanode which was coated with chiral molecules, had a lower overpotential for water oxidation and gave higher photocurrents. Figure 6 shows some of their results, in which they measured the H_2 yield. While at low overpotential (Fig. 6A) hydrogen is formed only when the anode is coated with chiral molecules, at high overpotential hydrogen can be formed also when the anode is coated with various achiral molecules (Fig. 6B). These observations are consistent with spin polarization of the OH radicals. More recently, they found that the production of hydrogen peroxide is suppressed by coating the photoanode with chiral molecules.[63] The production of the hydrogen peroxide depends on the overpotential and does not occur for lower potentials. As a result, even for the anode coated with

chiral molecules, the hydrogen production is less efficient at higher potentials than at the lower overpotential, as demonstrated in Fig. 6.

These observations imply that for multiple electron transfer processes in Nature, the chirality of the supramolecular assemblies (electron transfer system) may act to spin polarize the intermediates and affect the competition between different reaction pathways. A second example of biomolecules affecting the outcome of chemical reactions has been reported for enantioselectivity in the electron induced dissociation of (S)- and (R)-epichlorohydrin molecules, for which the electrons are spin polarized by self-assembled monolayers of duplex DNA.
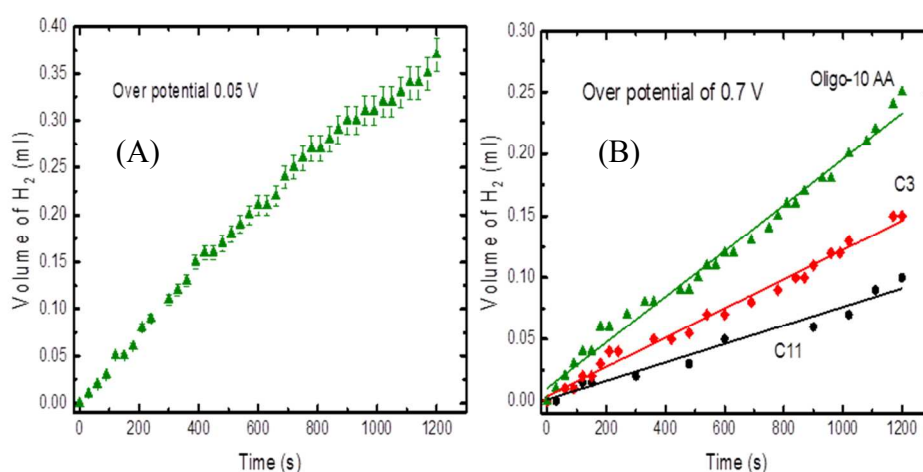

Figure 6: The hydrogen production as a function of time at two values of overpotential (versus Ag/AgCl electrode). Panel A shows the H_2 yield with time for an anode coated with the chiral oligopeptidet at low overpotential, and panel B shows the H_2 yields at higher overpotential for the anode coated either with the chiral oligopeptide or with achiral molecules. Copied with permission from reference 63.

4   Bio recognition

While the effects described above were already established experimentally, this section discusses an important implication of the CISS effect for enantioselective biorecognition processes. Biorecognition events are important for many biological processes, yet the high fidelity of enantioselective recognition remains a challenge to understand, and its calculation has evaded first principles theory.[64-67] Here, we propose a CISS based mechanism that can enhance the interaction strength between molecules of the same chirality over that for molecules of opposite chirality.

Non-covalent interactions between molecules in biological systems are commonly described by molecular force fields that are generated through a combination of quantum chemistry calculations and model fitting. As the molecules and molecular fragments used in such calculations are closed shell, spin effects are not typically included in the generation of such force fields. However, the interaction between two molecules necessarily involves some degree of charge polarization, and the transient 'current' associated with this charge polarization should give rise to a spin polarization, *via* the CISS effect. If this spin polarization affects the intermolecular interaction strength in a significant manner, then it could give rise to an intrinsic (arising from the chiral symmetry) enantioselectivity in the intermolecular interaction strength and ultimately affect the enantioselectivity in bio-recognition.

As an example, consider the interaction between two helical molecules as represented by the schematic diagram in Figure 7. When two molecules interact, charge polarization occurs. In the case of chiral molecules this charge polarization is accompanied by spin polarization, because of the CISS effect. Figure 7A shows the case of two molecules with the same helicity, for which the dynamic charge polarization (indicated by the asymmetric blue shading and the charge displacement q) also generates a spin polarization (indicated by the black arrows on the red balls). Because the molecules are of the same helicity (chirality), the spin polarization in the regions of enhanced electron density point in the same direction and the regions of depleted electron density point in the same, but opposite, directions. For the displacement shown in Fig 7A along the helical axis, the spin polarizations point outward along the helical axis. If the molecules are close enough together for sufficient electronic cloud overlap, then one must consider the exchange interaction between the molecules. For the case shown in Fig 7A the spin polarizations are aligned anti-parallel (paired like a singlet state); whereas for the case shown in Fig 7B for two interacting molecules of opposite chirality (represented by helices of opposite handedness) the spin polarizations have the opposite directions (pointed inward for the left handed helix whereas it is outward for the right handed helix). In this latter case the exchange interaction between the molecules is characterized by two spins parallel to each other, analogous to a triplet state, and this heterochiral interaction (Fig 7B) is more destabilizing than the homochiral interaction (Fig 7A). Another presentation of the same phenomenon is to say that a hole with one spin and an electron with opposite spin interact at the end of the chiral molecule, and that the hole attracts the electron of the opposite spin more strongly than it does an electron

of the same spin. In summary, this interaction between the spins is enantioselective; irrespective of its magnitude, it gives rise to an enantioselective force in Nature that is underappreciated.

How significant is the interaction energy? The difference in energy between the two cases results from the exchange integral in the Hamiltonian, and it can be on the order of an electron volt (96 kJ/mole) for large charge displacements, or a few percent of an electron volt for weak charge polarization.   It is important to appreciate that the exchange energy referred to here is coulombic, and not related to the weaker magnetic interaction energies of electrons. In principle, the exchange interaction is short range and decays with the distance between the electrons, as their orbital overlap decays. Hence, its contribution to the intermolecular forces will be at short range. Moreover, the spin polarization caused by the CISS effect is a dynamic phenomenon and occurs simultaneously with the charge polarization.
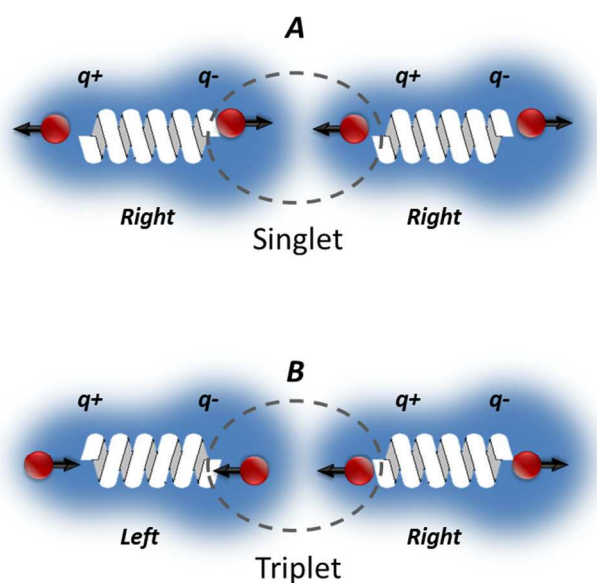

Figure 7: A) The diagram illustrates the interaction of two helices with the same handedness. Because of the induced dipole interaction charge *q* is transferred from one side of the helix to the other, and because of the CISS effect a spin polarization is generated (represented by a black arrow on the red ball). The side of the helix with excess electron density (*q-*) has a spin polarization parallel to the helical axis, and the side of the helix with a decrement of electron density (*q+*) has a spin polarization anti-parallel to the helical axis. In the region of electron density overlap (dotted circle-singlet surface), the two electron densities have a total spin polarization like that of a singlet state. B) When the helical charge distribution is of the opposite chirality, its spin polarization points in the opposite direction, hence the arrows are pointed inward for the left handed helix. For the two helices of opposite chirality the overlap region (in the dotted circle-triplet surface) is characterized by two spins parallel to each other, like a triplet state.

Once the flow of charge stops, the spin direction will randomize; however the spin depolarization in organic molecules, biomolecules included, can take microseconds or even longer. Once two molecules interact via the exchange interaction, the spin densities involved in the interaction would be locked relative to each other (aligned anti-parallel to each other as in Fig. 7A) and the spin randomization could be lengthened.

This type of force should exist only among chiral molecules and is expected to enhance the magnitude of homochiral interactions, by changing the repulsive part of the intermolecular potential. While the induced dipole-induced dipole nature of the interaction resembles dispersive forces like those first discussed by London,[68] they should not contribute significantly at long range, but rather they should contribute strongly at short range where orbital overlap is significant. It is known that something is missing from our current description of the interaction between biological molecules, this is evident from the lack of a chirality related interaction term and from the theoretical underestimation of affinities in biological systems.[69] The enantioselective interactions arising from the CISS effect may provide a theoretical basis for filling parts of this gap.

5 Conclusions

In this review, we described three processes arising from the chirality of molecules and specifically by the chiral induced spin selectivity (CISS) effect. We discussed studies which have been used to show that electron transfer through biomolecules can be highly efficient and spin selective, and we discussed how multi-electron reactions can have particular reaction pathways preferred by the spin filtering effect. In addition, we conjectured about a beneficial role that chiral induced spin selectivity might play in enantioselective biorecognition events. Each of these fundamental processes is important to Biology and the role played by spin and chirality is significant.

Acknowledgements

References

1 R. B. Perspect. *Biol. Med.* 1995, 38, 188-229.

2 E.N. Jacobsen, A. Pfaltz, H. Yamamoto, eds. 1999. *Comprehensive Asymmetric Catalysis.* Berlin: Springer 1214.

3 I. Ojima, ed. 2000. *Catalytic Asymmetric Synthesis*. New York: Wiley. 2nd ed.

4 T.P. Yoon, E.N. Jacobsen. *Scienc*e 2003, **299**,1691-93.

5 L.D. Barron. *Nature* 2000, **405**, 895-96.

6 R. Naaman, D. H. Waldeck, *Ann. Rev. Phys. Chem.* 2015, **66**, 263–81.

7 Z. Xie, T. Z. Markus, S. R. Cohen, Z. Vager, R. Gutierrez, R. Naaman, Nano Lett. 2011, **11**, 4652–4655.

8 R. A. Rosenberg, D. Mishra, R. Naaman, *Angew. Chemie*, 2015, **54**, 7295-7298.

9 M. Kettner, B. Göhler, H. Zacharias, D. Mishra, V. Kiran, and R. Naaman, C. Fontanesi, D. H. Waldeck, S. Sęk, J. Pawłowski J. Juhaniewicz *J. Phys. Chem. C* 2015, **119**, 14542−14547.

10 S. Ravi, P. Sowmiya, A. Karthikeyan, *Spin* 2013, **3**, 1350003.

11 K. M. Alam, S. Pramanik, *Adv. Func. Mat*. 2015, **25**,3210.

12 M. Á. Niño , I. A. Kowalik , F. J. Luque , D. Arvanitis , R. Miranda , J. J. Miguel, *Adv. Mater.* 2014, **26**, 7474–7479.

13 O. Ben Dor, N. Morali, S. Yochelis, L. T. Baczewski, Y. Paltiel, *Nano Lett*., 2014, **14**, 6042–6049.

14 N. Peer, I. Dujovne, S. Yochelis, Yossi Paltiel, *ACS Photonics*, 2015, **2**, 1476–1481.

15 L. Turin, E. M. C. Skoulakis, A. P. Horsfield, *Proc. Nat. Acad. Sci. USA*, 2014, **111**, E3524–E3533.

16 T. Koretsune, R. Arita, H. Aoki, *Phys. Rev. B* 2012, **86**,125207.

17 S. Yeganeh, M.A. Ratner, E. Medina, V. Mujica, *J. Chem. Phys*. 2009, **131**,014707.

18 E. Medina, F. Lopez, M.A. Ratner, V. Mujica, *Europhys. Lett.* 2012. **99**,17006.

19 a) R. Gutierrez, E. Díaz, R. Naaman, G. Cuniberti, *Phys. Rev. B* 2012, **85**, 081404. b) R. Gutierrez, E. Díaz, C. Gaul, T. Brumme, F. Domínguez-Adame, G. Cuniberti, *J. Phys. Chem. C* 2013, **117,** 22276-84.

20 a) A.M. Guo, Q.F. Sun, *Phys. Rev. Lett.* 2012, 108,218102. b) A.M. Guo, Q.F. Sun, Phys. *Rev. B* 2012, **86**, 115441 c) A.M. Guo, Q.F. Sun, *PNAS* 2014, **111**, 11658–11662.

21 A.A. Eremko, V.M. Loktev, *Phys. Rev. B* 2013, **88**,165409.

22 D. Rai, M. Galperin, *J. Phys. Chem. C* 2013, **117**, 13730-37.

23 J. Gersten, K. Kaasbjerg, A. Nitzan, *J. Chem. Phys.* 2013, **139**,114111.

24 S.L. Kuzmin, W.W. Duley, *Phys. Lett. A* 2014, **378**, 1674-50.

25 S. Matityahu, Y. Utsumi, A. Aharony, O. Entin-Wohlman, C. A. Balseiro, *Phys. Rev. B* 2016, **93**, 075407.

26 K. Michaeli, R. Naaman, arXiv:1512.03435v2 [cond-mat.mes-hall] 15 Jan 2016.

27 B. Göhler,V. Hamelbeck, T.Z. Markus, M. Kettner, G.F. Hanne, Z. Vager,

R. Naaman, H. Zacharias, *Science* 2011, **331**, 894-897.

28 S. Mayer, J. Kessler. *Phys. Rev. Lett.* 1995, **74,** 4803-4806.

29 M. Z. Hasan, C. L. Kane, *Rev. Mod. Phys*. 2010, **82**, 3045-3067.

30 M. Kai et. al. *J. Pept. Sci.* 2008, **14**, 192.

31 a) J. Juhaniewicz, J. Pawlowski, and S. Sek Isr. J Chem. 2015, **55,** 645-660; b) S. Sek et. al. *J. Phys. Chem. B* 2005, **109**, 18433,

32 J. Yu, J. R. Horsley, and A.D. Abell , Aust. J. Chem. 2013, **66**, 848–851

33. V. B. Engelkes , J. M. Beebe, C. D. Frisbie, *J. Am. Chem. Soc.,* 2004, **126**, 14287–14296.

34 J. F. Smalley, H. O. Finklea, C. E. D. Chidsey, M. R. Linford, S. E. Creager, J. P. Ferraris, K. Chalfant, T. Zawodzinsk, S. W. Feldberg, and M. D. Newton *J. Am. Chem. Soc* 2003, 125 , 2004-2013.

35 H. B. Gray, J. R. Winkler, *Annu Rev. Biochem* 1996, **65**, 537-61.

36 Y.-T. Long, E. Abu-Irhayem, Dr. H.-B. Kraatz, *Chem. Eur. J.* 2005, **11**, 5186 – 5194.

37 N. Amdursky *Chem Plus Chem* 2015, 80, 1075-1095.

38 J. R. Winkler and H. B. Gray *J. Am. Chem. Soc.* 2014, 136, 2930−2939

39. I. Carmeli, V. Skakalova, R. Naaman, Z. Vager, *Angewandte Chem. Int. Editi*on, 2002, **41**,761-764.

40 M. Eckshtain-Levi1, E. Capua, S. Refaely-Abramson, S. Sarkar, Y. Gavrilov, S. P. Mathew, Y. Paltiel, Y. Levy, L. Kronik, R. Naaman, *Nature Communica*tions 2016, **7**, 10744.

41 D. Mishra, T.Z. Markus, R. Naaman, M. Kettner, B. Göhler, H. Zacharias, N. Friedman, M. Sheves, C. Fontanesi, *PNAS* 2013, **110**, 14872–14876.

42 J. C. Genereux, S. M. Wuerth, J.K. Barton, *J. Am. Chem. Soc.* 2011, **133**, 3863–3868.

43 Y. Arikuma, H. Nakayama, T. Morita, S. Kimura, *Angew. Chem.* 2010, **122**, 1844 –1848.

44 X. Yu, R. Lovrincic, L. Sepunaru,W. Li, A. Vilan, I. Pecht, M. Sheves, D. Cahen, *ACS Nano* 2015, **9**, 9955–9963.

[45] A. Nitzan, J. Jortner, J. Wilkie, A. L. Burin, M A. Ratner, *J. Phys. Chem. B* 2000, **104**, 5661-5665.

46 a) J. Messinger and G. Renger, *Biochemistry*, 1994, **33**, 10896. b) J. Messinger, W. P. Schröder and G. Renger, *Biochemistry*, 1993, **32**, 7658.

47. W. Lubitz, E. J. Reijerse, J. Messinger, *Energy Environ. Sci*., 2008, **1**, 15–31.

48 J.O'M. Bockris, B. Dandapani, D. Cocke, J. Ghoroghchian, *International Journal of Hydrogen Energy* 1985, **10**, 179–201.

49 E. S. Andreiadis, M. Chavarot-Kerlidou, M. Fontecave, V. Artero, *Photochemistry and Photobiology* 2011, **87**, 946–964.

50 G. Renger, *J. Photochem. Photobiol. B* 2011, **104,** 35–43.

51 I. Carmeli, K. S. Kumar, O. Hieflero, C. Carmeli, R. Naaman, *Angew. Chemie* 2014, **53**, 8953 –8958.

52 G. P. Wiederrecht, M. Seibert, Govindjee, M. R. Wasielewski, *Proc. Nat. Acd. Sc. USA* **1994**, *91*, 8999-9003.

53 J. Deisenhofer, J. Norris, *Photosynthetic Reaction Center*, Academic Press, San Diego, CA, **1993**.

54. M. G. Müller, J. Niklas, W. Lubitz, A. R. Holzwarth, , *Biophysical J.* 2003, **85**, 3899–3922.

55 H. Makita, G. Hastings, *FEBS Letters* 2015, **589,** 1412–1417.

56 a) L. Frolov, Y. Rosenwaks, C. Carmeli, I. Carmeli, *Adv. Mater.* 2005, **17**, 2434 – 2437.

b) L. Frolov, Y. Rosenwaks, S. Richter, C. Carmeli, I. Carmeli, *J. Phys. Chem. C* 2008, **112**, 13426 – 13430.

57 K. S. Kumar, N. Kantor-Uriel, S. P. Mathew, R. Guliamov, R. Naaman, *Phys. Chem. Chem. Phys.*, 2013, **15**, 18357-18362.

58 M. C. Thurnauer, M. K. Bowman, J. R. Norris, *FEBS Lett*. 1979, **100**, 309-312.

59 G. C Dismukes, A. Mcguire, R. Blankenship, K. Sauer, *Biophysical J.* 1978, **21**, 239-256.

60 P. Gast, T. Swarthoff, F. C. R. Ebskamp, A. J. Hoff, *Biochim. Biophys. A*cta 1983, **722**, 163-175.

61 M. V. Rao, K. Rajeshwar, V. R. Pal Verneker, J. DuBow, *J. Phys. Chem*. 1980, **84**, 1987-1991.

62 W. Mtangi, V. Kiran, C. Fontanesi, R. Naaman, *J. Phys. Chem. Lett*., 2015, **6**, 4916–4922.

63 W. Mtangi, F. Tassinari, K. Vankayala, A. V. Jentzsch, B. Adelizzi, A. R.A. Palmans, C. Fontanesi, E.W. Meijer, R. Naaman, Submitted.

64. D. H. Williams, E. Stephens, D. P. O'Brien, M. Zhou, *Angew. Chem. Int. Ed.*, 2004, **43**, 6596– 6616.

65. M.Wilchek, E.A. Bayer, O. Livnah, *Immunology Letters*, 2006, **103,** 27-32.

66 U. Ryde, P. Söderhjelm, *Chem . Rev.* 2016 http://dx.doi.org/10.1021/acs.chemrev.5b00630.

67 J. R. Wagner, C. T. Lee, J.D. Durrant, R. D. Malmstrom, V. A. Feher, R. E. Amaro, *Chem. Rev.* 2016 http://dx.doi.org/10.1021/acs.chemrev.5b00631.

68 F. London, *Transactions of the Faraday Society* 1937, **33**, 8–26.

69 S. Ovchinnikov, et. al, *eLife 2*015, 10.7554/eLife.09248.